Jinzhe Gong, Mark L Stephens, Nicole S Arbon, Aaron C Zecchin, Martin F Lambert, and Angus R Simpson

On-site non-invasive condition assessment for cement mortar-lined metallic pipelines by time-domain fluid transient analysis

Structural Health Monitoring, 2015; 14(5):426-438

Published version available via DOI: http://dx.doi.org/10.1177/1475921715591875

On-site Non-invasive Condition Assessment for Cement Mortar Lined Metallic Pipelines by Time-Domain Fluid Transient Analysis

by

Gong, J., Stephens , M., Arbon, N., Zecchin, A.C., Lambert, M.F., and Simpson, A.R.

Journal of Structural Health Monitoring

Citation:
Gong, J., Stephens , M., Arbon, N., Zecchin, A.C., Lambert, M.F., and Simpson, A.R. (2015). "On-site Non-invasive Condition Assessment for Cement Mortar Lined Metallic Pipelines by Time-Domain Fluid Transient Analysis." *Journal of Structural Health Monitoring,* September, vol. 14, no. 5, 426-438. doi:10.1177/1475921715591875

For further information about this paper please email Angus Simpson at angus.simpson@adelaide.edu.au

On-site non-invasive condition assessment for cement mortar lined metallic pipelines by time-domain fluid transient analysis

Jinzhe Gong[1], Mark Stephens[2], Nicole Arbon[1], Aaron Zecchin[1], Martin Lambert[1], Angus Simpson[1]

[1]School of Civil, Environmental and Mining Engineering, the University of Adelaide, Adelaide, SA 5005, Australia

[2] South Australian Water Corporation, 250 Victoria Square, Adelaide, SA 5000, Australia

Corresponding author:

Jinzhe Gong, School of Civil, Environmental and Mining Engineering, the University of Adelaide, Adelaide, SA 5005, Australia

Tel: +61 (8) 8313 4323

Email: jinzhe.gong@adelaide.edu.au

Abstract

Pipeline condition assessment is essential to targeted and cost-effective maintenance of aging water transmission and distribution systems. This paper proposes a technique for fast and non-invasive assessment of the wall condition of cement mortar lined metallic pipelines using fluid transient pressure waves (water hammer waves). A step transient pressure wave can be generated by shutting off a side-discharge valve in a pressurised pipeline. The wave propagates along the pipe and reflections occur when it encounters sections of pipe with changes in wall thickness. The wave reflections can be measured by pressure transducers as they are indicative of the location and severity of the wall deterioration. A numerical analysis is conducted to obtain the relationship between the degree of change in wall thickness in a cement mortar lined pipe and the size of the corresponding pressure wave reflection. As a result, look-up charts are generated for any specific cement mortar lined pipeline to map this relationship. The wall thickness of a deteriorated or distinct section can be determined directly and quickly from the charts using the size of the reflected wave, thus facilitating on-site pipeline condition assessment. The validity of this time-domain pipeline condition assessment technique is verified by numerical simulations and a case study using the field data measured in a mild steel cement mortar lined (MSCL) water main in South Australia. The condition of the pipe as assessed by the proposed technique is generally consistent with ultrasonic measurements.

Keywords

on-site, non-invasive, pipeline condition assessment, fluid transient pressure wave, water transmission and distribution system, water hammer

Introduction

Water transmission and distribution pipelines are critical infrastructure for modern cities. Due to the sheer size of the networks and the fact that most pipelines are buried under ground, the health monitoring and maintenance of this infrastructure is challenging. Although a number of techniques have been developed for pipeline condition assessment, including visual inspection (e.g. closed-circuit television inspection[1]), electromagnetic methods (e.g. magnetic flux leakage method[2] and ground penetrating radar[3]), acoustic methods (e.g. SmartBall[4]), and ultrasonic methods (e.g. guided wave ultrasound inspection[5]), they are either too costly, inefficient for large networks or invasive [6]. Efficient and non-invasive pipeline condition assessment technologies are yet to be developed for targeted and cost-effective pipeline rehabilitation and the prevention of catastrophic events such as pipe failure.

Research in the past two decades has shown that fluid transients[7, 8], which are also known as water hammer waves, can be used for non-invasive detection of defects in pressurised pipeline systems. Fluid transients are pressure waves that propagate in the fluid and along a pipeline. A typical transient pressure wave used for detecting faults in pipelines is a step pressure wave generated by abruptly closing a side-discharge valve after the steady-state flow is established. Theoretically, any physical changes on the pipe wall, such as leaks or wall thinning due to corrosion, can introduce wave reflections. The reflected waves propagate towards the source of the initial transients (i.e. the side-discharge valve) and can be measured by pressure transducers installed on existing accessible points such as air valves or fire hydrants. The arrival time of the wave reflection can be used to determine the location of the defect, and the magnitude of the reflection is indicative of the severity of the deterioration[9].

Typical defects in aging pipelines include leaks, blockages, internal or external corrosion and the spalling of cement mortar lining in lined pipes. Leak detection using transient pressure waves has been a focus of research for many years and a number of techniques have been developed, either in the time domain[10-12], in the frequency domain[13-18], or by means of advanced signal processing (e.g. wavelet) that involves analysis in both domains[19-23]. Blockage detection has also been studied intensively, either for discrete blockages (orifices)[24-28] or extended partial blockages[29, 30]. The frequency-domain leak and blockage detection uses the change in the magnitude of resonant response or the shift of the resonant frequencies of the pipeline. The principle is similar to that used in vibration-based condition monitoring applied to other areas[31, 32].

In recent years, the use of fluid transients has been extended to non-invasively assess the condition of the pipe wall. Zecchin et al. [33, 34] studied general pipeline parameter identification using fluid transient waves but only limited to numerical analysis. Stephens et al.[35, 36] were the first to apply the inverse transient analysis (ITA) to detect degradation of the pipe wall in a mild steel cement mortar lined (MSCL) pipeline. The ITA uses an iterative process to calibrate pipeline parameters for a number of discretised reaches; therefore, it requires considerable computational effort for complex systems. Hachem and Schleiss[37] developed a technique for detecting a structurally weak section in a pipeline using a step transient pressure wave. The wave speed in the weak section was determined first and then the stiffness was estimated from the theoretical wave speed formula. However, challenges are expected when using their method to accurately determine wave speeds when multiple deteriorated sections exist in a pipeline. Gong et al.[9] proposed an approach for determining the wall thickness of a single degraded section in an unlined pipeline. It was found that the magnitude of the wave reflection resulting from a section with a uniform change in wall thickness was directly related to the hydraulic impedance of that section. The impedance could then be used to determine the wall thickness and wave speed in the degraded section. An advanced technique was then proposed by Gong et al.[38] to cater for the detection of multiple deteriorated sections in a pipeline. Only unlined pipelines were studied and the transient generation and measurement were required to be conducted at the upstream face of a closed end. However, in real water transmission systems, a great portion of pipelines used are cement mortar lined metallic pipes, and the requirement of generating and measuring at a closed end is not always achievable.

The research presented in this paper develops a technique that enables on-site condition assessment for cement mortar lined pipes by fast time-domain analysis of transient pressure wave reflections. The location of a defect with respect to the measurement point can be determined by time-domain reflectometry (TDR)[39] (i.e. using half the measured arrival time of the wave reflection multiplied by the wave speed). The procedure is not discussed in detail in this paper since applications have been reported in previous literature, such as for locating leaks[12, 20], partially closed in-line valves[27] and pipe sections with a thinner wall thickness[9]. The focus of this research is to achieve fast and quantitative determination of the wall thickness of a degraded section in a cement mortar lined pipe using the magnitude of the pressure wave reflection. Mild steel cement mortar lined (MSCL) pipe is studied in particular, but the analysis can be easily extended to any other types of metallic cement mortar lined pipes. Equations are derived to connect the degree of change in wall thickness of an MSCL pipe to the size of the corresponding wave reflection. Changes in wall thickness from either side of the pipe wall (internal or external) are considered. As a result, plots can be drawn to describe this relationship for any MSCL pipeline if the specifications of the intact part are known. These plots can be used as look-up charts for on-site transient-based pipeline condition assessment in practice. The validity of this new technique is verified by numerical simulations. The applicability of this technique is verified by conducting wall condition assessment using a transient pressure trace measured from a MSCL water main in South Australia. Significant wave reflections are selected using a threshold corresponding to full cement loss and then analysed using the look-up charts. The representative wall thicknesses are determined for four sections that are believed to have significant loss of the cement mortar lining and internal corrosion. The condition of the pipeline determined using the proposed technique is generally consistent with pipe wall ultrasonic thickness measurements.

Analysis of fluid transients in a cement mortar lined metallic pipe

This section discusses the relationship between the size of the reflected transient pressure wave and the degree of change in wall thickness in a cement mortar lined metallic pipeline. First, the typical measurement setup of the field test layout is outlined. Second, the fundamental equations are reviewed and then adapted to mild steel cement mortar lined (MSCL) pipes. Two scenarios are considered: an *internal* change and an *external* change in wall thickness.

Overview of Field Experiments

A typical configuration used for field measurement is given in Figure 1. A transient wave generator and multiple pressure transducers are typically used for each test. The adopted transient generator is a customised side-discharge valve connected to an existing access point (such as an air valve or scour valve). A small step transient pressure wave (typically 5 to 10 m in magnitude) is induced by rapidly closing (within 10 ms) the side-discharge valve after opening and releasing a flow (typically 20 to 40 L/s for pipes from 600 to 1000 mm in diameter) until steady-state conditions are reached. The generated incident wave then propagates along the pipe in both upstream and downstream directions. As discussed, reflections occur when the incident wave encounters a physical change in the pipe, such as a section with a reduction in wall thickness. The reflected waves propagate back towards the generator, and can be measured by pressure transducers that are mounted along the pipe (also at existing access points). The wave reflections are then able to be analysed to determine the location of defects from the arrival times, and the severity of the defects from the magnitude of the reflected wave. By comparing the arrival times of a specific reflection as measured by two or more pressure transducers at different locations, it can be determined whether the reflection comes from the upstream or downstream side of the generator.

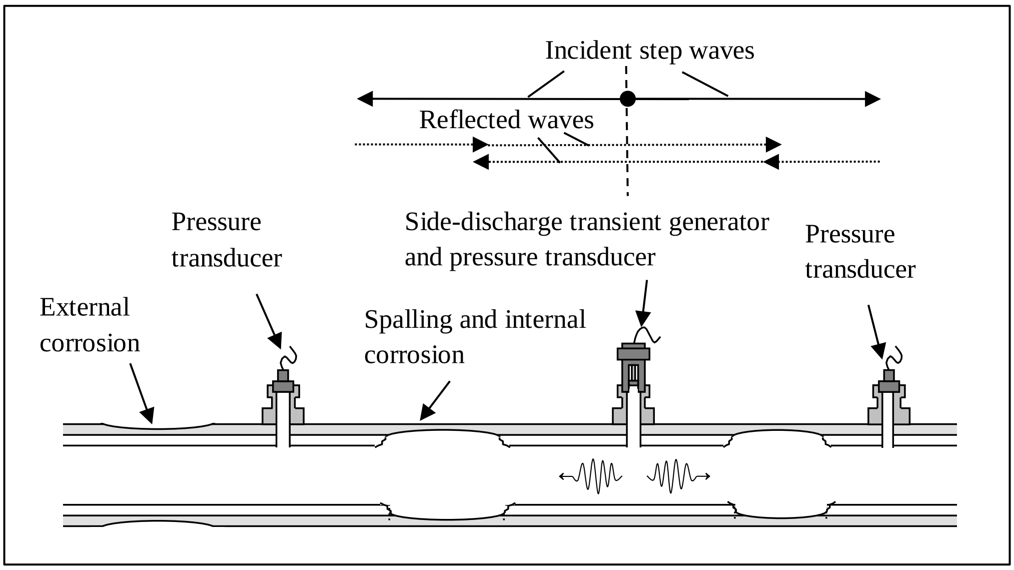

Figure 1. Typical configuration used in the field for pipeline condition assessment using transient pressure waves.

Fundamental equations

The spalling of cement mortar lining (CML) and extended internal, or external, corrosion are common problems in aging water pipelines. The deterioration often introduces a change in wall thickness, which in turn introduces a change in pipeline impedance. The impedance of a pipeline is defined as[7]

$$B = \frac{a}{gA} \tag{1}$$

where B is the impedance of the pipeline, a is the wave speed of pressure waves, g is the gravitational acceleration and A is the internal cross-sectional area of the pipe. The wave speed (a) can be determined using the theoretical wave speed formula[7, 8]

$$a^2 = \frac{K / \rho}{1 + (K / E)(D / e)c} \tag{2}$$

in which K is the bulk modulus of elasticity of fluid, ρ is the density of fluid, E is Young's modulus of the pipe wall material, D is the internal diameter of the pipeline, e is the wall thickness and c is a factor depending on the method of restraint of the pipeline[8].

Gong et al.[9] demonstrated that the size of the pressure wave reflection from a deteriorated pipe section is related to any change in the pipeline impedance of that deteriorated pipe section. The dimensionless head perturbation can be determined using

$$H_r^* = \frac{B_r - 1}{B_r + 1} \tag{3}$$

where H_r^* is the dimensionless head perturbation of the first reflected pressure wave and B_r is the ratio of the impedance of the deteriorated pipe section to the impedance of an intact section. The dimensionless head perturbation, H_r^* can also be defined from the incident and reflected transient waves as

$$H_r^* = \frac{H_{j1} - H_i}{H_i - H_0} \tag{4}$$

where H_{j1} is the head of the reflected pressure wave, H_i is the head of the incident transient pressure wave and H_0 is the steady-state head at the measurement point before the generation of the transient incident wave (during which time the side-discharge valve based transient generator is open). The values of H_{j1}, H_i and H_0 are measureable by a pressure transducer. Note that, although H_0 appears in Eq. (4), the dimensionless head perturbation H_r^* is independent from H_0. In addition, H_r^* is only related to the size of the reflection ($H_{j1} - H_i$, note that this can be negative) and the size of the incident wave ($H_i - H_0$). The impedance ratio B_r is given as

$$B_r = \frac{B_1}{B_0} \tag{5}$$

where the subscript '0' and '1' represent the intact pipe section and the section with a change in impedance (the deteriorated pipe section), respectively.

Equations adapted to mild steel cement mortar lined pipes

For pipelines with a cement mortar lining (CML), the contribution of the lining has to be considered when calculating the wave speed. Mild steel cement mortar lined (MSCL) pipe is used as an example to facilitate the analysis in this paper. The cross section of an intact MSCL pipe is shown diagrammatically in Figure 2.

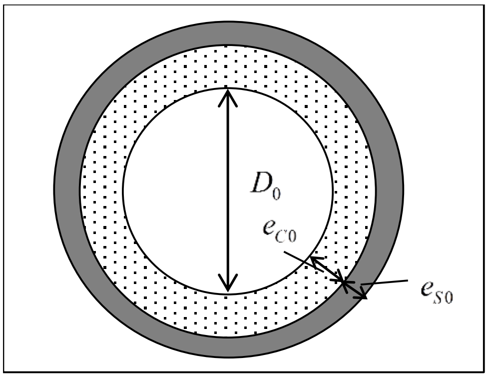

Figure 2. Cross section of an intact MSCL pipe (D_0 is the internal diameter of the pipe, e_{C0} is the thickness of the cement mortar lining and e_{S0} is the thickness of the steel pipe wall).

The cement mortar lining has a different modulus of elasticity to that of steel, but its contribution to the wave speed can be included as an equivalent thickness of steel[36]. The value of the total equivalent steel wall thickness ('equivalent steel thickness' as used in the rest of the paper) to be used in the wave speed formula is the summation of the equivalent thickness of steel contributed by the CML and the original thickness of the steel. For a thin-walled intact MSCL pipe, as shown in Figure 2, the equivalent steel thickness can be defined as e_0 and written as

$$e_0 = e_{C0}\frac{E_C}{E_S} + e_{S0} \tag{6}$$

where E_C and E_S are the modulus of elasticity of cement mortar lining and steel, respectively, and e_{C0} and e_{S0} are the thicknesses of the CML and that of the steel, respectively. The same concept of equivalent steel thickness was used in Wylie and Streeter[8] for reinforced concrete pipes. The use of the equivalent steel thickness [Eq. (6)] for thin-walled MSCL pipe is justified in the Appendix.

Assuming the same Poisson's ratio for steel and cement mortar, the theoretical wave speed for an intact MSCL pipe (Figure 2) is denoted as a_0 and can be written as

$$a_0^2 = \frac{K/\rho}{1+(K/E_S)(D_0/e_0)c} \tag{7}$$

where D_0 is the internal diameter of the intact MSCL pipe. Similarly, the wave speed in a section with a change in wall thickness can be written as

$$a_1^2 = \frac{K/\rho}{1+(K/E_S)(D_1/e_1)c} \tag{8}$$

where a_1, D_1 and e_1 are the wave speed, the internal diameter and the equivalent steel thickness, in the section with a change in wall thickness, respectively. As a result, B_r can be re-expressed as

$$B_r = \frac{a_1 D_0^2}{a_0 D_1^2} \tag{9}$$

To facilitate the analysis in subsequent sections, the relative change in equivalent steel thickness , e_{rc} , is given as

$$e_{rc} = \frac{e_1 - e_0}{e_0} \tag{10}$$

The aim of this research is to develop algorithms for estimating the remaining wall thickness of a deteriorated section from a measured transient pressure trace. For any pipeline, wall deterioration or a change in wall thickness (which results in a change in impedance) can occur either internally or externally or both. Theoretically, there are three possibilities for the cement mortar lining: intact, change in thickness (internally) and total loss. There are also three possibilities for the steel wall: intact, external change in thickness and internal change in thickness. As a result, there are 9 theoretical combinations for the condition of the pipe wall. Internal wall deterioration (only) and external wall deterioration (only) are discussed in subsequent sections. Simultaneous internal and external wall deterioration is not discussed in this paper, but it is expected to require a superposition of the effects caused by internal wall deterioration (only) and external wall deterioration (only).

Four commonly-seen wall deterioration cases are identified as illustrated in Figure 3: (a) $S1$: an internal change in the thickness of the CML; (b) $S2$: total loss of the CML plus an internal reduction in the thickness of the steel wall; (c) $S3$: intact CML with an internal change in the thickness of the steel wall; and (d) $S4$: intact CML with an external change in the thickness of the steel. Case $S3$ exists when the pipeline was initially installed with no lining but lined after years, or a section of original pipe is replaced by a section in the same nominal size (same outside diameter) but a different class (with thicker or thinner steel wall), or sections of a different class are installed during construction.

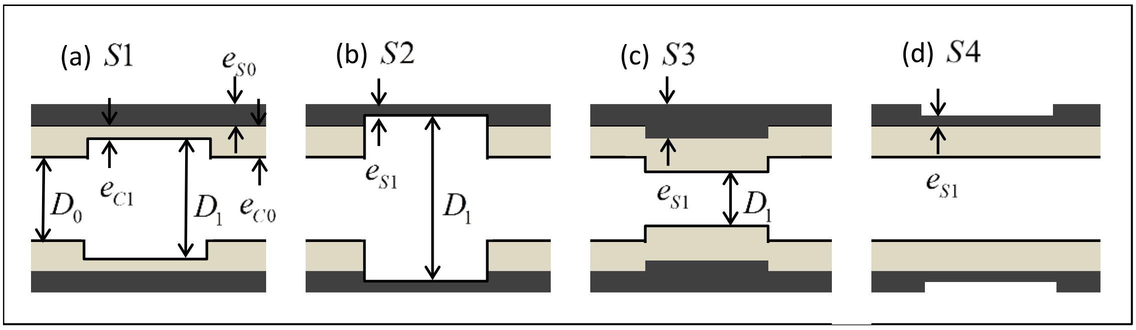

Figure 3. Longitudinal view of four sections of MSCL pipe with the changes in wall thickness considered in this research: (a) $S1$: an internal change in the thickness of the CML; (b) $S2$: total loss of the CML plus an internal reduction in the thickness of the steel wall; (c) $S3$: intact CML with an internal change in the thickness of the steel wall; and (d) $S4$: intact CML with an external change in the thickness of the steel wall.

An internal change in wall thickness

For the scenario of an internal change in wall thickness, the diameter and wall thickness of the intact and damaged sections can be related based on the fact that the external diameter is constant. If the change is in the thickness of the CML alone [$S1$, Figure 3(a)], the following equation holds

$$D_0 + 2e_{C0} = D_1 + 2e_{C1} \tag{11}$$

where e_{C1} is the thickness of the CML in the deteriorated/distinct section. In this case, the total equivalent steel thickness is given as

$$e_1 = e_{C1}\frac{E_C}{E_S} + e_{S0} \tag{12}$$

Substituting Eqs. (6) and (12) to Eq. (11) yields

$$D_0 + 2e_0\frac{E_S}{E_C} = D_1 + 2e_1\frac{E_S}{E_C} \tag{13}$$

Substituting e_1 as given in Eq. (10) into Eq. (13), the ratio D_1 / e_1 can be written as

$$\frac{D_1}{e_1} = \frac{D_0}{e_0(1+e_{rc})} - 2\frac{E_S}{E_C}\frac{e_{rc}}{1+e_{rc}} \tag{14}$$

Substituting Eq. (14) into Eq. (8), and then substituting the ratio D_0 / e_0 using Eq. (7), the wave speed a_1 can be described by

$$a_1^2 = \frac{(K/\rho)\left(1+e_{rc}\right)a_0^2}{(K/\rho)+e_{rc}a_0^2\left(1-2cK/E_C\right)} \tag{15}$$

Substituting e_1 as given in Eq. (10) into Eq. (14) and rearranging the subsequent equation yields

$$\frac{D_0}{D_1} = \frac{1}{1-2e_{rc}\left(e_0/D_0\right)\left(E_S/E_C\right)} \tag{16}$$

Substituting Eqs (15) and (16) into Eq. (9), and replacing D_0 / e_0 with an expression including a_0 as given in Eq. (7), the impedance ratio can be described by

$$B_r = \sqrt{\frac{(K/\rho)\left(1+e_{rc}\right)}{(K/\rho)+e_{rc}a_0^2\left(1-2c\,K/E_C\right)}}\left[1-2e_{rc}\frac{\left(K/E_C\right)a_0^2c}{K/\rho-a_0^2}\right]^{-2} \tag{17}$$

Where finally, substituting Eq. (17) into Eq. (3), the relationship between the dimensionless head perturbation of the first reflected pressure wave H_r^* and the relative change in equivalent steel thickness e_{rc} for case $S1$ can be obtained as

$$H_r^* = \frac{\sqrt{\dfrac{(K/\rho)(1+e_{rc})}{(K/\rho)+e_{rc}a_0^2(1-2cK/E_C)}} - \left[1-2e_{rc}\dfrac{(K/E_C)a_0^2c}{K/\rho-a_0^2}\right]^2}{\sqrt{\dfrac{(K/\rho)(1+e_{rc})}{(K/\rho)+e_{rc}a_0^2(1-2cK/E_C)}} + \left[1-2e_{rc}\dfrac{(K/E_C)a_0^2c}{K/\rho-a_0^2}\right]^2} \tag{18}$$

It can be seen from Eq. (18) that the dimensionless head perturbation H_r^* is related to the relative change in the equivalent steel thickness e_{rc}, the wave speed in the intact pipeline a_0, and physical properties of the pipeline and fluid that are typically known (K and ρ). The value of a_0 can be calculated using the theoretical formula in Eq. (7), or measured by conducting experiments. As a result, when conducting pipeline condition assessment, the value of e_{rc} can be determined from the value of H_r^*, which in turn can be determined from a measured transient pressure trace. A curve describing values of H_r^* corresponding to values of e_{rc} can be plotted numerically. An example will be presented in the *numerical simulations* section.

Eq. (18) is for an internal change in the thickness of the CML. A negative value of e_{rc} represents a thinning in CML, which can be induced by deterioration. In this research, positive e_{rc} is also considered, which represents a section of pipe with a CML thickness greater than the standard thickness. The lower bound of e_{rc} is reached when the CML is totally lost and is calculated as e_{S0}/e_0-1.

For case $S2$ in Figure 3(b), the relationship between H_r^* and e_{rc} can be determined by a similar procedure as used in the derivation of Eqs (11) to (18). The expression of H_r^* for the $S2$ case is given by

$$H_r^* = \frac{\sqrt{\dfrac{(K/\rho)(1+e_{rc})}{K/\rho + e_{rc}a_0^2 - 2ca_0^2 K\left(1/E_C - 1/E_S\right)\left(e_{S0}/e_0 - 1\right)}} - \left\{1 - 2\dfrac{(K/E_S)a_0^2 c}{K/\rho - a_0^2}\left[e_{rc} + \left(\dfrac{E_S}{E_C} - 1\right)\left(\dfrac{e_{S0}}{e_0} - 1\right)\right]\right\}^2}{\sqrt{\dfrac{(K/\rho)(1+e_{rc})}{K/\rho + e_{rc}a_0^2 - 2ca_0^2 K\left(1/E_C - 1/E_S\right)\left(e_{S0}/e_0 - 1\right)}} + \left\{1 - 2\dfrac{(K/E_S)a_0^2 c}{K/\rho - a_0^2}\left[e_{rc} + \left(\dfrac{E_S}{E_C} - 1\right)\left(\dfrac{e_{S0}}{e_0} - 1\right)\right]\right\}^2} \tag{19}$$

Note that the value of $2cK/E_S$ is in the order of 10^{-2} so that an approximation $1-2cK/E_S \approx 1$ is used in the derivation of Eq. (19). The possible range of e_{rc} is from -1 to $e_{S0}/e_0 - 1$. The lower bound corresponds to total loss of the CML plus total reduction of the steel wall, and the upper bound refers to total loss of the CML, but no reduction in the steel thickness.

By combining Eqs (18) and (19), a curve can be plotted for any specific MSCL pipe to describe the relationship between H_r^* and e_{rc} for cases $S1$ and $S2$ together. A discontinuity is expected in the curve, which represents the situation of total loss of the CML, but no loss of the steel wall thickness.

Case $S3$, i.e. intact CML with an internal change in the thickness of the steel wall, can be analysed by the same strategy as used for cases $S1$ and $S2$. Analysis shows that case $S3$ is equivalent to the scenario of an internal change in wall thickness in an unlined pipe. Using the approximation of $1-2cK/E_S \approx 1$, the relationship between H_r^* and e_{rc} in this case is given by

$$H_r^* = \frac{\sqrt{\dfrac{(K/\rho)(1+e_{rc})}{K/\rho + e_{rc}a_0^2}} - \left[1 - 2e_{rc}\dfrac{(K/E)a_0^2 c}{K/\rho - a_0^2}\right]^2}{\sqrt{\dfrac{(K/\rho)(1+e_{rc})}{K/\rho + e_{rc}a_0^2}} + \left[1 - 2e_{rc}\dfrac{(K/E)a_0^2 c}{K/\rho - a_0^2}\right]^2} \tag{20}$$

An external change in wall thickness

Case $S4$ shown in Figure 3(d), i.e. intact CML with an external change in the thickness of the steel wall, is discussed in this subsection. An example is a pipe section with a reduction in wall thickness due to extended external corrosion.

The equivalent steel thickness for case $S4$ can be written as

$$e_1 = e_{C0}\frac{E_C}{E_S} + e_{S1} \tag{21}$$

The intact pipe and the section with an external change in wall thickness have the same internal diameter D_0. As a result, in this case, D_0 can be used in the formula for a_1 [Eq. (8)] and B_r is the ratio of the wave speeds, i.e. $B_r = a_1/a_0$. Using Eqs (7), (8), (10) and (21), the impedance ratio can then be derived as

$$B_r = \sqrt{\frac{(K/\rho)(1+e_{rc})}{(K/\rho)+e_{rc}a_0^2}} \tag{22}$$

Substituting Eq. (22) into Eq. (3) results

$$H_r^* = \frac{\sqrt{(K/\rho)(1+e_{rc})} - \sqrt{(K/\rho)+e_{rc}a_0^2}}{\sqrt{(K/\rho)(1+e_{rc})} + \sqrt{(K/\rho)+e_{rc}a_0^2}} \tag{23}$$

In Eq. (23), the lower bound of e_{rc} is $-e_{S0}/e_0$, which represents total loss of the steel wall. A curve can be drawn for a specific MSCL pipeline for Eq. (23), and it can serve as a look-up chart for pipeline condition assessment.

Numerical simulations

Numerical simulations using the Method of Characteristics (MOC)[7, 8] were conducted to verify the validity of Eqs. (18), (19), (20) and (23). A reservoir-pipeline-valve (RPV) system was studied and a step transient pressure wave was used as the excitation. The physical details of the pipeline are those for the existing MSCL Morgan Transmission Pipeline (MTP) in South Australia, which will be further discussed in the subsequent *case study* section. For intact sections, the external diameter is 762 mm, the internal diameter (D_0) is 727.5 mm, the thickness of the CML (e_{C0}) is 12.5 mm and the thickness of the steel (e_{S0}) is 4.76 mm. Other parameters used in the numerical study include: the estimated elastic modulus of the cement mortar E_C = 25 GPa; the elastic modulus of the steel pipe wall E_S = 210 GPa; the bulk modulus of water (at 15℃) K = 2.14 GPa; the density of water (at 15℃) ρ = 999.1 kg/m^3 and the restraint factor for an axially and laterally restrained steel pipe c = 0.91 (for a Poisson's ratio for the steel pipe wall of 0.3). As a result, the theoretical wave speed and equivalent steel thickness for an intact section are calculated as a_0 = 1015 m/s and e_0 = 6.25 mm, respectively.

Plots for Eqs. (18), (19), (20) and (23) can be drawn using the physical details of the intact MSCL pipeline. Curves of Eqs. (18) and (19) are shown together in Figure 4. The point at $e_{rc} = e_{S0} / e_0 - 1$ = −0.238 and H_r^* = −0.076 is the intersection of the curves of Eqs. (18) and (19) and it corresponds to total CML loss with an intact steel wall. Plots for Eqs (20) and (23) are given in Figure 5 and Figure 6. The lower bound for the curve in Figure 6 is $e_{rc} = -e_{S0} / e_0$ = −0.762. Figures 4 to 6 can be used as look-up charts for pipeline condition assessment for the MTP.

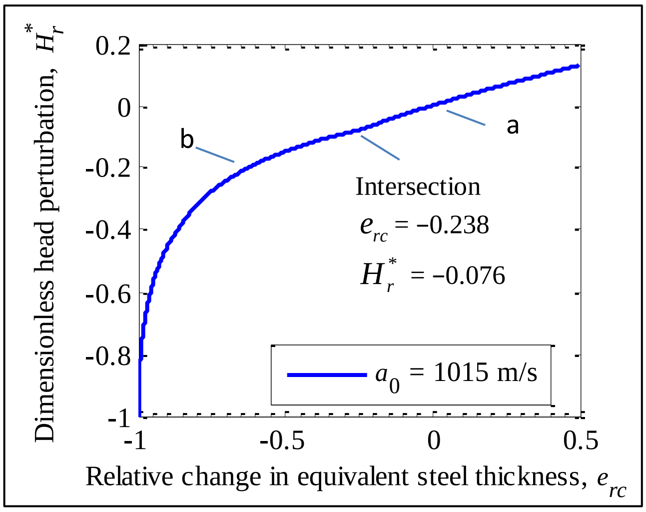

Figure 4. Relationship between the dimensionless head perturbation (H_r^*) and the relative change in equivalent steel thickness (e_{rc}) for: (a) an internal change in the thickness of the CML [Eq. (18), $S1$ in Figure 3(a)], and (b) total loss of the CML plus a reduction in the thickness of the steel wall [Eq. (19), $S2$ in Figure 3(b)].

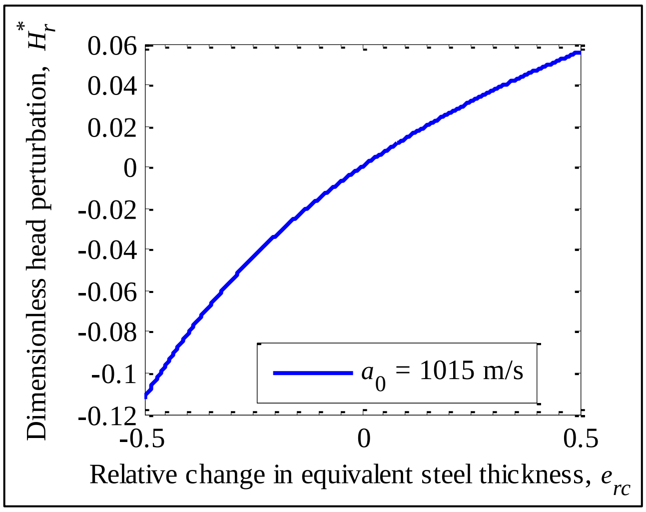

Figure 5. Relationship between the dimensionless head perturbation (H_r^*) and the relative change in equivalent steel thickness (e_{rc}) for the case of intact CML with an internal change in the thickness of the steel wall [Eq. 20, $S3$ in Figure 3(c)].

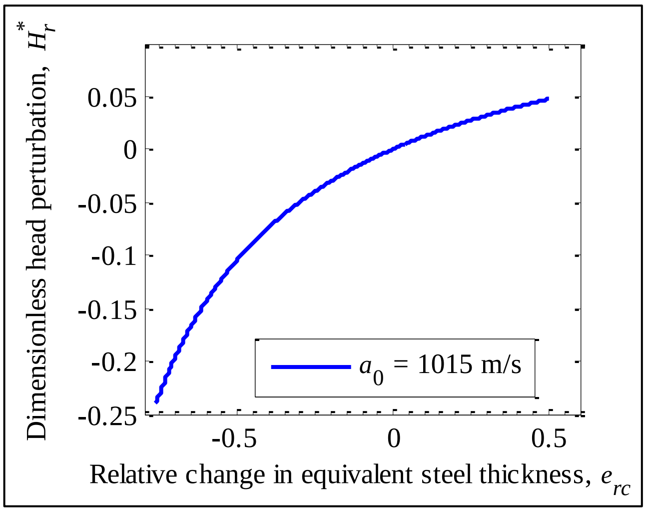

Figure 6. Relationship between the dimensionless head perturbation (H_r^*) and the relative change in equivalent steel thickness (e_{rc}) for an external change in the thickness of the steel wall [Eq. (23), $S4$ in Figure 3(d)].

The four cases, $S1$ to $S4$ as shown in Figure 3, are simulated by MOC in sequence and independently (i.e. in each simulation, only one case was involved). Specifically, the sections of pipe involved in the simulations include: (a) $S1$: e_{C1} = 6 mm; (b) $S2$: e_{S1} = 3 mm; (c) $S3$: e_{S1} = 6.35 mm; and (d) $S4$: e_{S1} = 3 mm. A reservoir-pipeline-valve system was used and the total length of the pipeline was taken as 2333 m. The length of each section with a change in wall thickness was approximately 100 m (with slight adjustment to keep the Courant number value to unity) and started from 1015 m downstream of the reservoir. The time step used in the MOC was 0.0005 s. A step transient wave was generated by closing the downstream valve within one time step. Friction was not considered in the MOC simulations. Pressure responses were measured at a point 203 m downstream from the deteriorated section.

The theoretical wave speeds in the four sections ($S1$ to $S4$) were calculated using the wave speed formula with the results: a_{1_S1} = 975 m/s, a_{1_S2} = 801 m/s, a_{1_S3} = 1074 m/s, and a_{1_S4} = 925 m/s. The theoretical equivalent steel thicknesses for the four sections ($S1$ to $S4$) were calculated as e_{1_S1} = 5.47 mm, e_{1_S2} = 3.0 mm, e_{1_S3} = 7.84 mm, e_{1_S4} = 4.49 mm. The theoretical relative changes in the equivalent steel thicknesses are calculated as e_{rc_S1} = −0.124, e_{rc_S2} = −0.520, e_{rc_S3} = 0.254, e_{rc_S4} = −0.282.

The dimensionless head perturbations (H_r^*) obtained from the MOC simulations for the four cases are given in Figure 7. The values of the dimensionless head perturbations are also shown in Figure 7.

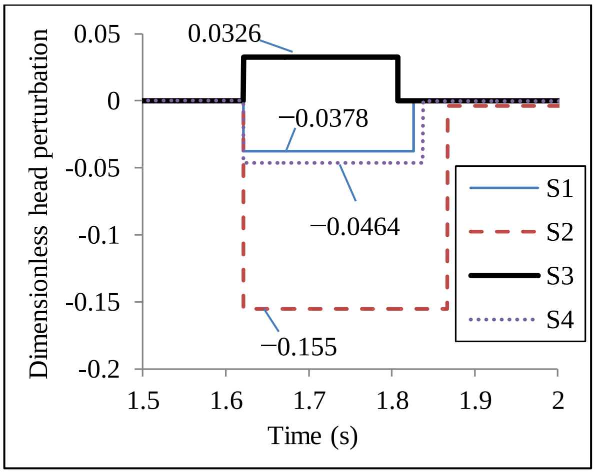

Figure 7. Dimensionless head perturbations obtained from the MOC simulations for the four pipe sections with changes in wall thickness ($S1$ to $S4$).

Using Figures 4 to 6, the corresponding values for the relative change in the equivalent steel thickness can be determined for each case, and the results are $e_{rc\_S1}^{MOC} = -0.123$, $e_{rc\_S2}^{MOC} = -0.519$, $e_{rc\_S3}^{MOC} = 0.258$, $e_{rc\_S4}^{MOC} = -0.283$. It can be seen that the results determined from the numerical transient pressure traces are consistent to a high degree with the analytical results (e_{rc_S1} to e_{rc_S4}). The small differences are from rounding errors and the approximations used in the derivation of Eqs. (18), (19), (20) and (23). The numerical simulations verify that Eqs (18), (19), (20) and (23) are valid, and they can be used for quantitative pipeline condition assessment. For a specific measured wave reflection, potential deterioration scenarios can be listed and the remaining wall thickness for each scenario can be determined.

Case study

A real-world case study is conducted to verify the applicability of the proposed pipeline condition assessment technique. A section of pipe in the Morgan Transmission Pipeline (MTP) in South Australia is studied. The section of pipe studied in this paper is from chainage (location as measured along the pipe length from some datum) 15000 m to CH 18000 m, covering scour valve No. 24 (SV24), and air valves No. 43 (AV43) and No. 44 (AV44). The layout of the section of pipe under study is given in Figure 8.

The MTP is an above ground MSCL water main between a pump station and a staging tank over a length of 26.1 km. During the field testing, the pump was turned off and formed a dead-end boundary. The pipeline system was pressurised by the staging tank. The physical details for intact pipe sections (D_0 , e_{C0} , e_{S0} , e_0 and a_0) and other parameters (E_C , E_S , K , ρ and c) have been given in the section *numerical simulations*. The section between CH 15735 m and CH 15840 m has a known thicker steel thickness of 6.35 mm. However, the external diameter and the thickness of the CML in this section are the same as counterparts in the original intact sections (Case $S3$). A few replacements with thicker steel wall are also located in this section of pipe. These replacement sections are not considered here because of their short length (typically a few meters). A transient generator, which is a customised side-discharge valve, was used at SV24 to produce step transient pressure waves. Flow meters were connected to the side-discharge valve to measure the steady-state side-discharge before the signal generation. The steady-state side-discharge is used to facilitate the determination of the magnitude of the incident step wave. Pressure transducers were placed at SC24, AV43 and AV44 to measure the pressure response. More details about the field tests and an analysis of this section of pipe using inverse transient analysis (ITA) are given in Stephens et al. [36].

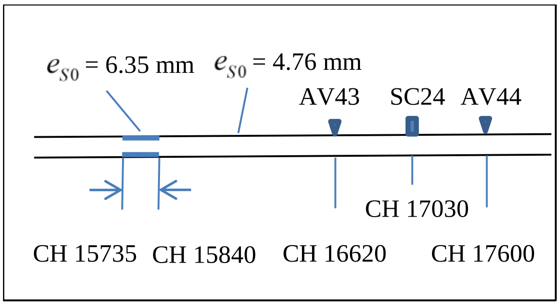

Figure 8. Layout of a section of the Morgan transmission pipeline.

The dimensionless head perturbations between chainage 15000 m and 16500 m, as measured at AV43, are shown in Figure 9 as the solid line. Long-period (low frequency) pressure oscillations associated with the opening of the side-discharge valve (to introduce a side-discharge) have been removed by a band-pass filter and the original pressure trace and filtered trace are presented in Stephens et al.[36]. The steady-state head is determined by averaging a short period of the data measured before the arrival of the incident wave, and the result is H_0 = 32.01 m. The magnitude of the incident wave ($H_i - H_0$) is estimated from the wave front shown in the measured trace (the range from the steady state head H_0 to the first peak shown on the top of the wave front, which is 37.80 m), and the result is 5.79 m.

The x-axis in Figure 9 is the chainage corresponding to the wave reflections. The chainage information is obtained by time-domain reflectometry (TDR) and using the measured arrival time of the reflection and the representative wave speeds. The arrival time of a reflection as measured by a transducer (relative to the arrival time of the wave front) is the time for a pressure wave to travel to, and be reflected back from, the corresponding defect. The representative wave speed for the section between AV43 (CH16620) and the right boundary of the thicker-walled section (CH15840) is 930 m/s, which is determined by the known distance and the arrival time of the reflection resulting from the thicker-walled section. The representative wave speeds for the thicker-walled section and the pipe section on its left side are calculated as 1050 m/s and 900 m/s respectively.

The dashed line in Figure 9 represents the value of the dimensionless head perturbation resulting from a section of pipe with total CML loss but intact steel wall, which is H_r^* = −0.076. This dashed line acts as a threshold to distinguish significant reflections that result from deteriorated sections with total CML loss and internal corrosion. The steel wall thickness values were also measured by an ultrasonic thickness measurement instrument at 5 m intervals along the MTP between CH 14900 and CH 18900. The ultrasonic measurements were taken at eight points around the circumference of the pipe (P1 to P8, starting from the top of the pipe and with 45° interval around the circumference) at each location. The interval of measurement was reduced to 1 m for some sections where changes in steel wall thickness were detected. The dotted line in Figure 9 gives the average steel wall thickness along the section of pipe (average of the ultrasonic wall thicknesses measurements at eight points around the circumference). The markers shown in Figure 9 are ultrasonic measurements of the steel wall thickness with values less than 4.3 mm (this value is considered significant as it corresponds to approximately a 10% steel wall reduction compared to the original steel thickness of 4.76 mm as given by the manufacturer for an intact MSCL section).

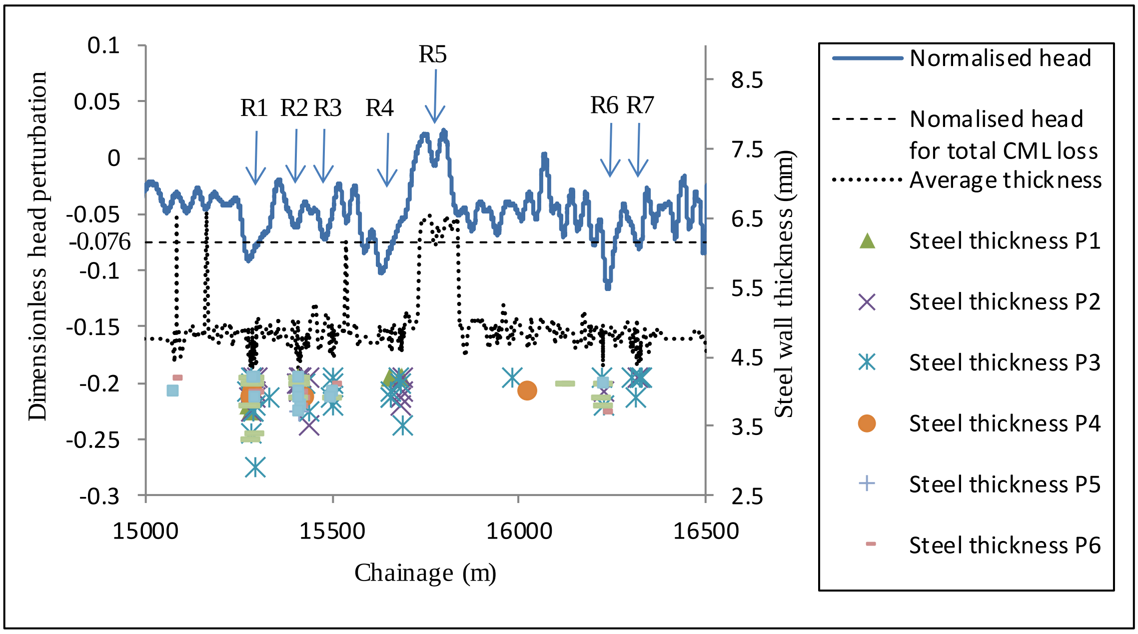

Figure 9. Dimensionless head perturbation (as function of distance) measured at AV43 (the solid line), dimensionless head perturbation resulting from a section of pipe with total CML loss but intact steel wall (the dashed line), average steel thickness measured by ultrasonic sounding (the dotted line), and ultrasonic measurements with values less than 4.3 mm (marks as indicated in the legend).

Seven significant reflections are selected for analysis, shown as R1 to R7 in Figure 9. The selection is based on a comprehensive analysis of the transient traces measured at AV43, SC24 and AV44 in the same test to ensure the selected reflections are induced by defects that are located on the left hand side of AV43 (see Figure 8). A reflection coming from the left hand side of AV43 will appear in the trace measured at

AV43 first, then shows at SC24 and finally arrives at AV44. The time lag between the arrival times of a reflection is consistent with the time for the initial incident pressure wave traveling from one point to another. By moving the traces measured at SC24 and AV44 forward in time by the corresponding time lag and then plotting them together with that measured at AV43, reflections from the left hand side of AV43 are overlapped while reflections from the other direction are not, consequently enabling an identification of the directional source of the reflection.

The reflection R5 is from a known feature, the thicker-walled section between CH 15735 m and CH 15840 m, and it aligns with Case S3 as in Figure 3(c). The maximum dimensionless head perturbation for R5 is read as 0.0254 from Figure 9. Using the look-up chart given in Figure 5, the relative change in equivalent steel thickness is determined as 0.195. Using Eq. (10) and e_0 = 6.25 mm for the MTP, the equivalent steel thickness for this thicker-walled section is determined as e_1^{R5} = 7.47 mm. Using Eq. (6) and e_{C0} = 12.5 mm for the MTP, the thickness of the steel wall for the thicker-walled section is determined as e_{S1}^{R5} = 5.98 mm. This result is smaller than the steel wall thickness given by the manufacturer for this section (which was 6.35 mm) and the ultrasonic measurement (6.1 to 6.5 mm). The discrepancy is believed to be caused by the inaccuracy of the estimated magnitude of the dimensionless head perturbation for R5 and the damping of the transient pressure wave.

The MTP is an above ground pipe and no significant external wall deterioration was observed during the testing for the pipe section under study. As a result, the reflections R1 to R4, R6 and R7 are believed to be associated with pipe sections with internal changes in wall thicknesses. In real MSCL pipelines, the internal wall deterioration is more complex than the situation discussed in the numerical study [Cases S1 and S2 as shown in Figure 3(a) and (b)]. The deterioration of CML mainly includes cracking, de-bonding, and spalling, and the distribution of deterioration is not uniform around the internal circumference. This has been confirmed by the CCTV camera footage obtained for the MTP and photo evidence has been included in Stephens et al[36]. After spalling of the CML, internal corrosion may start on the steel wall. The sizes of the dimensionless reflections are compared with the threshold that represents uniform total CML loss (dashed line in Figure 9).. Reflections R1, R4, R6 and R7 are greater than the threshold so that they are believed to be indications of large scale CML loss together with considerable internal corrosion of the steel wall. Reflections R2 and R3 are significant but haven't reached the threshold, so that they are indications of considerable de-bonding and spalling of the CML and likely to be associated with localised internal corrosion.

To quantify the deterioration, the look-up chart in Figure 4 is used to determine the representative wall thickness (the remaining wall thickness under uniform wall deterioration assumption). Sections associated with reflections R1, R4, R6 and R7 are equivalent to sections with total CML loss and uniform thinning of the steel wall (Case $S2$), in which the representative remaining steel wall thicknesses are determined as e_{S1}^{R1} = 4.34 mm, e_{S1}^{R4} = 4.05 mm, e_{S1}^{R6} = 3.76 mm and e_{S1}^{R7} = 4.62 mm, respectively. Note that the results are only the representative steel wall thicknesses (based on the assumption of 'uniform deterioration') and the thicknesses in some patches can be smaller than the representative values. Because the damping of the transient wave (which reduces the magnitude of wave reflections) is approximately proportional to the distance travelled by the wave, and the reflections R1 to R4 are resulting from sections more than 1 km away from the measurement point (AV43), the condition of these sections is likely to be worse than the representative conditions as determined by using the observed magnitudes of the reflections.

Overall, the condition of the pipe, as determined by applying the proposed technique, is generally consistent with the ultrasonic results of the steel wall thickness. Six pipe sections with significant internal wall deterioration are identified by using the dimensionless head perturbation trace and the representative steel wall thicknesses are determined by the look-up charts. The case study demonstrates that the proposed pipeline condition assessment technique can be used for non-invasive condition assessment for cement mortar lined pipes in the field.

Limitations and challenges

The proposed pipeline condition assessment technique has been proven to be useful but it has its limitations and some challenges are expected in the field. This time-domain technique directly maps the magnitude of a wave reflection to the wall thickness, which makes the technique efficient and easy to use, but also limits its application to the interpretation of selected significant wave reflections only. In contrast, the inverse transient analysis (ITA) is much more complex to apply, but it can provide information for the whole section of pipe under test and to a much higher resolution[36].

Internal and external changes in wall thickness are analysed separately in this research and equations that describe the relationship between a wave reflection and an internal or external change in wall thickness have been derived respectively. However, from a measured transient pressure trace, it is difficult to tell if a reflection is due to an internal or an external change in wall thickness. Without additional information, the operator has to estimate the wall thicknesses for different scenarios. If priori information is available (for example, from visual inspections of an above ground pipe), the operator can firstly determine the most likely wall deterioration scenario and then choose the corresponding look-up chart for the estimation of the remaining wall thickness.

The accuracy of the look-up chart based technique proposed in this paper relies on the accurate determination of the wave speed for the intact pipe (a_0) and the magnitude of the dimensionless head perturbation as induced by the deteriorated section. In real pipelines, the determined a_0 may have uncertainties since some physical properties of the pipeline may be unknown; deterioration is more likely to be non-uniform; multiple deteriorated sections can introduce overlapped complex reflections; and the transmission of the transient pressure wave is subject to signal dissipation and dispersion. These practical challenges make the accurate estimation of the dimensionless head perturbation difficult. Provided the dimensionless head perturbation is determined with acceptable accuracy, the wall thickness as obtained from the look-up chart is the representative wall thickness that indicates the overall condition of the deteriorated section. Localised information about wall thickness, such as the remaining steel thickness of a corrosion pit, is unable to be determined.

The sharpness of the incident pressure wave is important[40], but the generation of a sharp and clean step transient incident pressure wave in real pipelines is a challenge. In the case study reported in this paper, a ball valve-based side-discharge valve was connected to the downstream of a scour valve to act as the transient generator and the closing time was typically less than 10 ms[36]. As a result, the generated incident pressure wave was sharp and the pressure oscillation in the scour valve chamber damped out in less than 30 ms. However, in cases where the generator cannot be connected to the main pipe closely but via a relatively long stand pipe (e.g. several meters), the pressure oscillations in the stand pipe after the valve closure can be significant and persist for a longer time (hundreds of milliseconds), which impedes the analysis of the measured transient pressure signal for that time period. If the side-discharge valve is not closed quickly enough so that the wave front is not as sharp as the step wave used in the numerical analysis, the reflections from the deterioration will not be sharp either. This may lead to error in the determination of the remaining wall thickness of a deteriorated section if the length of the section is shorter than $T_r a / 2$, where T_r is the rise time of the wave front. A numerical study presented in Gong et al.[9] explores how the sharpness of a wave front affects the accuracy of the analysis.

Despite the limitations and challenges, the proposed technique is efficient and applicable to condition assessment of cement mortar lined pipes in the field. The accuracy of the determination of the wall thickness can be improved in the future if techniques are developed to compensate the effects of multiple reflections and signal damping.

Conclusions

A new technique has been developed in this paper for the condition assessment of cement mortar lined pressurised pipes. The condition assessment is achieved by time-domain analysis of the transient pressure wave reflections measured at existing access points along a pipeline, such as air valves. The relationship between a change in wall thickness (either internal or external) in a cement mortar lined metallic pipe and the size of the wave reflection has been derived analytically for the first time. As a result, plots can be drawn to describe the relationship for any specific pipeline and these plots can serve as look-up charts for transient-based pipeline condition assessment. Numerical simulations have been conducted to verify the validity of the analytical findings. A case study has been conducted on a section of mild steel cement mortar lined (MSCL) water main in South Australia to illustrate how to apply the proposed technique to field data and also verify its applicability. The dimensionless head perturbation trace as measured at an air valve has been plotted and analysed. A threshold value, which represents the dimensionless head perturbation that would be induced by a section of pipe with total loss of the cement mortar lining, is used to facilitate evaluation of the significance of the wave reflections. Seven significant transient reflections have been identified and analysed, with one from a known thicker-walled section and the other six from sections with considerable internal wall deterioration. The reflection from the known feature and the four reflections that have magnitudes greater than the threshold are further analysed using the look-up chart to determine the representative thicknesses of the steel wall. The results are generally consistent with the ultrasonic measurements.

This technique is non-invasive as fluid transient waves are used as the tool for the detection of defects. This technique is also efficient as look-up charts are used and no interactive calculation is involved. The proposed technique enables on-site transient-based condition assessment for cement mortar line metallic pipes, which is cost-effective and contributes to strategic maintenance of critical pipeline assets.

Acknowledgements

The research presented in this paper has been supported by the Australian Research Council through the Linkage Project Grant LP130100567.

Appendix

Justification of the total equivalent steel wall thickness (equivalent steel thickness) as defined in Eq. (6) and used in Eq. (7)

For a pressure wave propagating inside a frictionless pipe with uniform cross section, classic one-dimensional water hammer theory gives the general wave speed formula as[8]

$$a = \sqrt{\frac{K/\rho}{1 + (K/A)(\Delta A/\Delta p)}} \quad \text{(A1)}$$

where ΔA is the variation of the cross-sectional area of the pipe caused by the variation of the water pressure Δp. For a thin-walled steel pipe with thin-walled cement mortar lining, the change in tensile stress in the steel wall and in the cement mortar lining, $\Delta\sigma_S$ and $\Delta\sigma_C$ respectively as illustrated in Figure A1, are related to the change in radial force induced by Δp, where the relationship is

$$\Delta\sigma_S e_{S0} + \Delta\sigma_C e_{C0} = \Delta p D_0 / 2 \quad \text{(A2)}$$

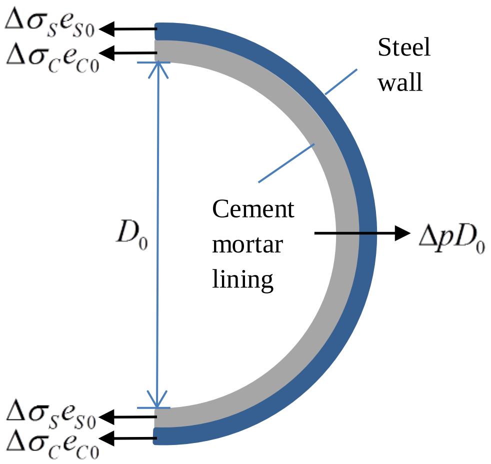

Figure A1. Forces on semicylinder of pipe due to variation in pressure.

Assuming the cement mortar lining is closely bonded with the steel wall so that the change in circumferential unit strain is the same in both layers, ignoring the change in axial tensile stress and applying Hooke's law to Eq. (A2), the change in circumferential unit strain $\Delta\varepsilon$ can be written by

$$\Delta\varepsilon = \frac{\Delta p D_0}{2\left(E_C e_{C0} + E_S e_{S0}\right)} \tag{A3}$$

The radial extension is obtained by multiplying $\Delta\varepsilon$ by the radius $D_0 / 2$, which , when multiplied by πD_0, yields the change in cross sectional-area ΔA. As a result, the following equation is derived:

$$\frac{\Delta A}{A \Delta p} = \frac{D_0}{E_C e_{C0} + E_S e_{S0}} \tag{A4}$$

Substituting Eq. (A4) into Eq. (A1) and applying mathematical manipulation, the wave speed is given by

$$a = \sqrt{\frac{K/\rho}{1+(K/E_S)(D_0/e_0)}} \quad \text{(A5)}$$

where e_0 is the total equivalent steel wall thickness (equivalent steel thickness) as defined by Eq. (6). If e_{S0} = 0 (no steel wall) and e_{C0} = 0 (no cement lining), Eq. (A5) becomes the commonly seen general wave speed formula for uniform material thin-walled elastic pipe. If E_S or E_C reaches infinity, Eq. (A5) becomes $a = \sqrt{K/\rho}$, which is the acoustic speed of a small disturbance in an infinite fluid.

If the change in axial tensile stress is considered, the Poisson's ratio can be used to describe the relationship between the circumferential strain and the axial strain. Assuming that the Poisson's ratios are the same for steel and cement, Eq. (7) can be derived.

References

1. Jo BY, Laven K and Jacob B. Advances in CCTV technology for in-service water mains. *Pipelines 2010: Climbing New Peaks to Infrastructure Reliability - Renew, Rehab, and Reinvest, August 28, 2010 - September 1, 2010*. Keystone, CO, United states: American Society of Civil Engineers, 2010, p. 538-47.
2. Grimes J and De Alvarez AN. Utilizing circumferential MFL for the detection of linear and axially oriented metal loss anomalies in pipelines. *2008 ASME International Pipeline Conference, IPC 2008, September 29, 2008 - October 3, 2008*. Calgary, AB, Canada: American Society of Mechanical Engineers, 2009, p. 401-11.
3. Ekes C, Neducza B and Henrich GR. Completing condition assessments using in-pipe GPR as pipe penetrating radar. *Pipelines 2011: A Sound Conduit for Sharing Solutions*. Seattle, WA, United States: ASCE, 2011, p. 693-703.
4. Paulson P and Nguyen V. Pipe wall evaluation using acoustic pulses. *Pipelines 2010: Climbing New Peaks to Infrastructure Reliability - Renew, Rehab, and Reinvest, August 28, 2010 - September 1, 2010*. Keystone, CO, United states: American Society of Civil Engineers, 2010, p. 711-8.
5. Lowe MJS, Alleyne DN and Cawley P. Defect detection in pipes using guided waves. *Ultrasonics*. 1998; 36: 147-54.
6. Liu Z and Kleiner Y. State of the art review of inspection technologies for condition assessment of water pipes. *Measurement*. 2013; 46: 1-15.
7. Chaudhry MH. *Applied Hydraulic Transients*. 3rd ed. New York, NY: Springer, 2014.

8. Wylie EB and Streeter VL. *Fluid Transients in Systems*. Englewood Cliffs, New Jersey, USA: Prentice Hall Inc., 1993, p.463.

9. Gong J, Simpson AR, Lambert MF, Zecchin AC, Kim Y and Tijsseling AS. Detection of distributed deterioration in single pipes using transient reflections. *J Pipeline Syst Eng Prac*. 2013; 4: 32-40.

10. Jönsson L and Larson M. Leak detection through hydraulic transient analysis. In: Coulbeck B and Evans EP, (eds.). *In Pipeline Systems*. Dordrecht, the Netherlands Kluwer Academic Publishers, 1992, p. 273-86.

11. Brunone B and Ferrante M. Detecting leaks in pressurised pipes by means of transients. *J Hydraulic Res*. 2001; 39: 539-47.

12. Lee PJ, Lambert MF, Simpson AR, Vítkovský JP and Misiunas D. Leak location in single pipelines using transient reflections. *Australian Journal of Water Resources*. 2007; 11: 53-65.

13. Sattar AM and Chaudhry MH. Leak detection in pipelines by frequency response method. *J Hydraulic Res*. 2008; 46: 138-51.

14. Mpesha W, Gassman SL and Chaudhry MH. Leak detection in pipes by frequency response method. *J Hydraulic Eng*. 2001; 127: 134-47.

15. Covas D, Ramos H and Betamio de Almeida A. Standing wave difference method for leak detection in pipeline systems. *J Hydraulic Eng*. 2005; 131: 1106-16.

16. Lee PJ, Vítkovský JP, Lambert MF, Simpson AR and Liggett JA. Leak location using the pattern of the frequency response diagram in pipelines: a numerical study. *J Sound Vib*. 2005; 284: 1051–73.

17. Gong J, Lambert MF, Simpson AR and Zecchin AC. Single-event leak detection in pipeline using first three resonant responses. *J Hydraulic Eng*. 2013; 139: 645-55.

18. Duan H-F, Lee PJ, Ghidaoui MS and Tung Y-K. Leak detection in complex series pipelines by using the system frequency response method. *J Hydraulic Res*. 2011; 49: 213-21.

19. Urbanek J, Barszcz T, Uhl T, Staszewski W, Beck S and Schmidt B. Leak detection in gas pipelines using wavelet-based filtering. *Struct Health Monit*. 2012; 11: 405-12.

20. Ferrante M and Brunone B. Pipe system diagnosis and leak detection by unsteady-state tests. 2. wavelet analysis. *Adv Water Resour*. 2003; 26: 107-16.

21. Ghazali MF, Staszewski WWJ, Shucksmith JD, Boxall JB and Beck SBM. Instantaneous phase and frequency for the detection of leaks and features in a pipeline system. *Struct Health Monit*. 2011; 10: 351-60.

22. Taghvaei M, Beck SBM and Boxall JB. Leak detection in pipes using induced water hammer pulses and cepstrum analysis. *Int J COMADEM*. 2010; 13: 19-25.

23. Ferrante M, Brunone B and Meniconi S. Leak-edge detection. *J Hydraulic Res*. 2009; 47: 233-41.

24. Lee PJ, Vítkovský JP, Lambert MF, Simpson AR and Liggett JA. Discrete blockage detection in pipelines using the frequency response diagram: numerical study. *J Hydraulic Eng*. 2008; 134: 658-63.

25. Mohapatra PK, Chaudhry MH, Kassem AA and Moloo J. Detection of partial blockage in single pipelines. *J Hydraulic Eng*. 2006; 132: 200-6.

26. Sattar AM, Chaudhry MH and Kassem AA. Partial blockage detection in pipelines by frequency response method. *J Hydraulic Eng*. 2008; 134: 76-89.

27. Meniconi S, Brunone B and Ferrante M. In-line pipe device checking by short-period analysis of transient tests. *J Hydraulic Eng*. 2011; 137: 713-22.

28. Brunone B, Ferrante M and Meniconi S. Discussion of "Detection of partial blockage in single pipelines" by P. K. Mohapatra, M. H. Chaudhry, A. A. Kassem, and J. Moloo. *J Hydraulic Eng*. 2008; 134: 872-4.

29. Duan H-F, Lee PJ, Ghidaoui MS and Tung Y-K. Extended blockage detection in pipelines by using the system frequency response analysis. *J Water Resour Plan Manage*. 2012; 138: 55-62.

30. Meniconi S, Duan HF, Lee PJ, Brunone B, Ghidaoui MS and Ferrante M. Experimental investigation of coupled frequency and time-domain transient test-based techniques for partial blockage detection in pipelines. *J Hydraulic Eng*. 2013; 139: 1033-44.
31. Carden EP and Fanning P. Vibration based condition monitoring: a review. *Struct Health Monit*. 2004; 3: 355-77.
32. Wei Fan and Pizhong Qiao. Vibration-based damage identification methods: a review and comparative study. *Struct Health Monit*. 2011; 10: 83-111.
33. Zecchin AC, White LB, Lambert MF and Simpson AR. Parameter identification of fluid line networks by frequency-domain maximum likelihood estimation. *Mech Syst Signal Pr*. 2013; 37: 370-87.
34. Zecchin A, Lambert M, Simpson A and White L. Parameter identification in pipeline networks: transient-based expectation-maximization approach for systems containing unknown boundary conditions. *J Hydraulic Eng*. 2014; 140: 04014020.
35. Stephens ML, Simpson AR and Lambert MF. Internal wall condition assessment for water pipelines using inverse transient analysis. In: Van Zyl JE, Ilemobade, A.A., Jacobs, H.E., (ed.). *10th Annual Symposium on Water Distribution Systems Analysis (WDSA 2008)*. Kruger National Park, South Africa: ASCE, 2008.
36. Stephens ML, Lambert MF and Simpson AR. Determining the internal wall condition of a water pipeline in the field using an inverse transient model. *J Hydraulic Eng*. 2013; 139: 310–24.
37. Hachem FE and Schleiss AJ. Detection of local wall stiffness drop in steel-lined pressure tunnels and shafts of hydroelectric power plants using steep pressure wave excitation and wavelet decomposition. *J Hydraulic Eng*. 2012; 138: 35-45.
38. Gong J, Lambert MF, Simpson AR and Zecchin AC. Detection of localized deterioration distributed along single pipelines by reconstructive MOC analysis. *J Hydraulic Eng*. 2014; 140: 190-8.
39. Furse C, Chung Y, Lo C and Pendayala P. A critical comparison of reflectometry methods for location of wiring faults. *Smart Struct Syst*. 2006; 2: 25-46.
40. Meniconi S, Brunone B, Ferrante M and Massari C. Small amplitude sharp pressure waves to diagnose pipe systems. *Water Resour Manage*. 2010; 25: 79-96.